Hindawi
Advances in Materials Science and Engineering
Volume 2022, Article ID 3225574, 12 pages
https://doi.org/10.1155/2022/3225574

Research Article

High-Volume Upcycling of Waste Sediment and Enhancement Mechanisms in Blended Grouting Material

Luchen Zhang,[1] **Xuena Jia**,[1] **Guanjie Yang**,[2] **and Deming Wang**[1]

[1]*School of Transportation and Civil Engineering, Shandong Jiaotong University, Jinan 250357, China*
[2]*The Second Construction Limited Company, China Construction Eighth Engineering Division, Jinan 250014, China*

Correspondence should be addressed to Xuena Jia; jiaxuena1023@163.com

Received 23 December 2021; Revised 8 January 2022; Accepted 15 January 2022; Published 31 January 2022

Academic Editor: Yonghong Wang

Waste sediment (WS) is a solid waste produced from subway construction. In the present work, high-volume WS was upcycled to prepare grouting material.The results showed that the working performances (consistency, fluidity, setting time, bleeding ratio, and stone ratio)of WS-based grouting material were significantly affected by the mass concentration of solid components, binder to WS ratio, and steel slag addition. This material can meet the engineering requirement by adjusting these parameters. The WS-based grouting material exhibited superior performance compared to traditional grouting materials. It achieved self-leveling (160 mm fluidity) and wassuitable for grouting (consistency within 100-130 mm, 95.0% stone ratio). Amorphous phases were formed in the hardened sample. The addition of a suitable amount of steel slag (10%) can reduce the total porosity, and also promote the hydration degree and increase the mechanical properties of cement matrix.The strength development can be attributed to the formation of hydration products and the cementation between hydrates and sediment particles.

1. Introduction

The shield method is commonly applied in current subway construction. As an urban underground transportation project, shield subway tunnels should be durable and safe [1, 2]. When the shield machine works, the surrounding soil is disturbed. A 90~140 mm annular gap is formed between the segment and the soil when the segment is about to be removed from the shield [3]. In order to prevent settlement and segment offset, the gap must be filled by grouting material so that the surrounding rock can be supported in time to control formation deformation, ensure the stability of the segment, and prevent floating [4, 5]. Synchronous grouting closely adheres the stratum to the segment, and the surrounding stratum produces uniform pressure on the segment through the early strength of the grouting layer, which improves the safety of the segment in shield subway tunnels [6, 7].

Nowadays, the demand for high-fluidity synchronous grouting materials is becoming increasingly urgent. The grouting material needs to have good fluidity, suitable setting time, excellent stability, and small shrinkage rate [8, 9]. It must have sufficient strength to support the stratum, prevent settlement deformation, and control the rise of the segment. Moreover, the grouting material also requires excellent anti-seepage ability, which can reduce water seepage problems, control ground settlement, and ensure construction safety [10, 11]. However, the currently used grouting materials in shield engineering have some shortcomings. Development of grouting materials that can adapt to specific engineering needs has become a research hotspot [12, 13].

Waste sediment is produced during the excavation of subway construction. It is a kind of solid waste, which has caused massive pressure on the urban environment [14, 15]. At present, the waste sediment is mainly transported to the designated landfill area. The transportation volume is large, and it is easy to cause environmental pollution [16]. Besides, the cost of processing waste sediment accounts for about 10% of the cost of the subway construction [17, 18]. Thus, the utilization of the waste sediment is an important task.

In recent years, some researchers have explored ways to reuse the waste sediment [19, 20]. A mud separation treatment technology has been applied to separate the mud into soil and water, and reuse the soil [21, 22]. The existing mud water treatment equipment has been modified according to different stratum conditions, and suitable measures such as a filter press system and centrifuge system have been added to solve the problem of environmental pollution caused by the waste mud generated by the mud water shield construction [23, 24]. The solid-liquid separation method can slightly reduce the discharge of waste sediment, but the amount of sediment absorption is still limited [25]. Hence, some researchers have tried to use the waste sediment for shield grouting tests [26]. Waste sediment has been used instead of water and bentonite to prepare the grouting material. It was found that the layering degree and bleeding rate of the synchronous grouting slurry prepared with waste sediment were significantly reduced, which solved the pumping problem occurring during grouting [27, 28]. The initial fluidity of the grouting material is about 230 mm, and the 28-day compressive strength is greater than 2.5 MPa, meeting the property requirement in the grouting field [29, 30].

The preparation of synchronous grouting materials is a feasible way to utilize the waste sediment, which can reduce environmental pollution, manpower waste, and material resources [26, 31]. At present, researchers have carried out some exploratory experiments on the preparation of grouting materials from waste sediment and carried out specific engineering applications. However, the preparation of grouting materials from the waste sediment of subway projects is closely related to the quality of the ground and the performance requirements of the grouting materials in shield engineering. Besides, some researchers have dried and ground waste sediment before preparing the cement brick, which is a low-efficiency method with high energy consumption [29]. At present, few studies have been conducted on the preparation of grouting materials using the untreated waste sediment produced from the subway constructionin Jinan city, Shandong province.

Hence, in the current research, the waste sediment produced from the subway construction in Jinan city, Shandong province, was directly utilized to prepare the grouting material. Steel slag, which is a solid waste produced in the power generation industry, was also used to partially replace cement, aiming to reduce the cost and protect the environment. The consistency, fluidity, setting time, bleeding ratio, and stone ratio of the fresh slurry were analyzed. For the hardened sample, the compressive strength and pH value were tested. Analysis methods such as X-ray diffraction (XRD), scanning electron microscopy (SEM), and mercury intrusion porosimetry (MIP) was used to observe the microstructureand analyze the hydrate formation. The current research results would be helpful to prepare suitable grouting materials from the waste sediment in an ecofriendly way, to solve the water inrush problem in subway constructions and significantly reduce environmental pollution caused by waste sediment.

2. Materials and methods

2.1. Raw Materials. Ordinary Portland cement (OPC, 42.5 grade) was produced by Huaxin cement plant in Hubei province, which had a specific surface area of 412 m^2/kg. Steel slag (SL) was obtained from a power plant in Jinan city, with specific surface area of 435 m^2/kg. The waste sediment (WS) was produced during the subway construction in Jinan city. It was sorted and utilized by the centrifugal dehydration method. The chemical compositions of these three raw materialsare listed in Table 1. As seen fromthe SEM images in Figure 1, OPC and SL mainly consisted of small square-shaped particles, while WS particles had an irregular shape. The flocculated small particles in WS are responsible forits high water absorption ratio.

Table 2 presents the basic physical properties of the waste sediment. It contained 25.1% water and 41.5% sand. The liquid limit and plastic limit were 42.3 and 24.6, respectively. The plasticity index was 17.7. The pH value of the waste sediment was 6.91. After drying, the particle size distribution of the waste sediment was analyzed, and the results are listed in Table 3.

2.2. Sample preparation. Table 4 lists the mix proportions of the waste sediment-based grouting material. When using waste sediment to prepare the grouting material, the water contained in waste sediment should be considered. This part of the water should be included when calculating the mass concentration of solid components (binder and waste sediment) in the slurry. Insamples S1 to S5, different mass concentrations(69%, 67%, 65%, 63%, and 61%) of solid components were applied to prepare the slurry, in order to study the effect of mass concentration on the performance of waste sediment-based grouting material and determine the optimal mass concentration. In samples S3, S6, S7, S8, S9, S10, and S11, the binder to waste sediment (WS) mass ratio was changed from 2/1 to 1/6, aiming to explore the effect of binder to waste sediment ratio and determine the suitable proportion in the waste sediment-based grouting material. Finally, in samples S9, S12, S13, S14, S15, and S16, the addition amount of steel slag (SL) was increased from 0% to 50%, in order to study the effect of steel slag.

In this study, the weighed raw materials were added to the mixer and mixed for 3 min. Then, water was added and mixed evenly for 4 min. The consistency, fluidity, setting time, bleeding ratio, and stone ratio of the fresh slurry were tested immediately after mixing. The fresh slurry was poured into a mold and cast under standard conditions (temperature of 20±2 °C and relative humidity of 95±2%).

2.3. Testing methods. The consistency and setting time were tested based on JGJ/T 70. The penetration resistance method was used to determine the setting time, and the ZKS-100 mortar consistency meter was applied to test the consistency. The fluidity was measured according to GB/T 50448. The bleeding ratio and stone ratio of the fresh slurry were analyzed according to T/CECS 563-2018. The photos of fluidity, consistency, and bleeding ratio tests are displayed in

Table 1: Chemical compositions of raw materials.

Raw material	Chemical composition (%)								
	CaO	SiO_2	Al_2O_3	Fe_2O_3	MgO	K_2O	Na_2O	SO_3	LOI
OPC	63.47	21.71	4.32	4.61	1.12	0.41	0.12	1.24	1.84
SL	46.11	15.36	2.12	18.02	9.91	0.21	0.11	0.65	1.78
WS	3.02	64.11	16.01	2.34	2.15	2.16	1.87	1.82	2.56

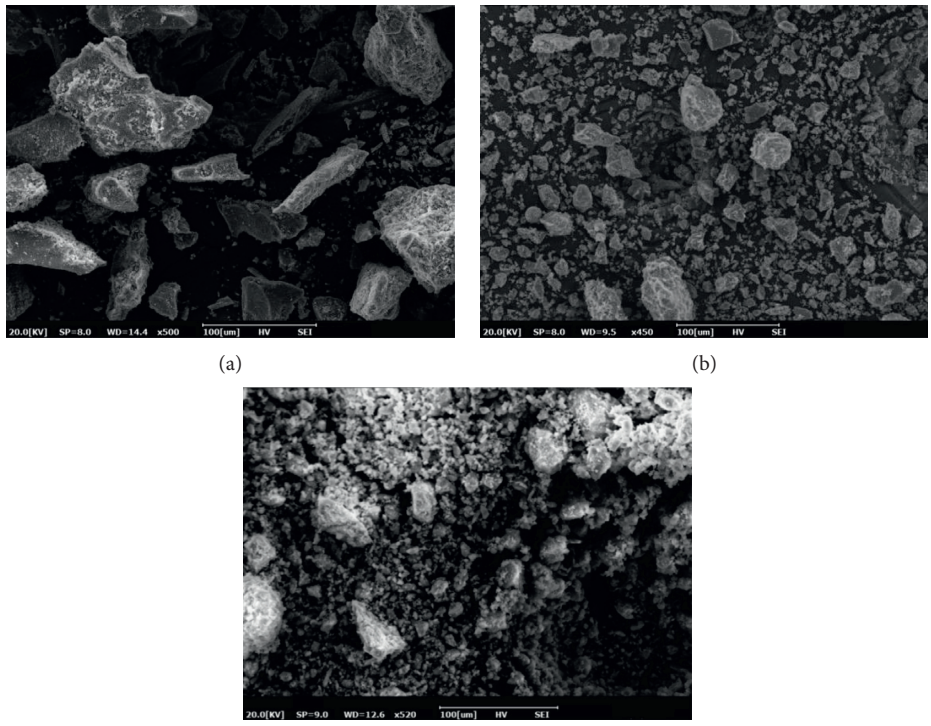

(a) (b) (c)

Figure 1: SEM observation of raw materials: (a) OPC; (b) SL; and (c) WS.

Table 2: Basic physical properties of the waste sediment.

Property	Value
Initial water content (wt%)	25.1
Sand content (%)	41.5
Liquid limit (%)	42.3
Plastic limit (%)	24.6
pH value	6.91

Table 3: Particle size distribution of the waste sediment.

Particle size (mm)	<0.001	0.001-0.01	0.01-0.10	0.10-0.50	>0.50
Percentage (%)	1.6	3.4	54.5	36.7	3.8

Figure 2. Parallel experiments were carried out for each group to ensure the accuracy of the test data.

The compressive strength of the hardened sample was measured according to GB/T 17671-2005. The size of the

Table 4: Mix proportions of the waste sediment-based grouting material (wt%).

Group	Mass concentration	Binder/WS	SL/binder
S1	69%	1/1	0%
S2	67%	1/1	0%
S3	65%	1/1	0%
S4	63%	1/1	0%
S5	61%	1/1	0%
S6	65%	2/1	0%
S7	65%	1/2	0%
S8	65%	1/3	0%
S9	65%	1/4	0%
S10	65%	1/5	0%
S11	65%	1/6	0%
S12	65%	1/4	10%
S13	65%	1/4	20%
S14	65%	1/4	30%
S15	65%	1/4	40%
S16	65%	1/4	50%

Note. mass concentration: mass ratio of solid component (binder and WS); binder: mass of OPC and SL.

(a) (b) (c)

Figure 2: Tests on fresh grouting materials: (a) fluidity; (b) consistency; and (c) bleeding ratio.

sample was 40 mm×40 mm×160 mm. The sample was split into two sections through the flexural test, and then the compressive strength test was conducted. The pH value of the hardened sample after curing for 28 days was tested according to GB/T 50123-1999. During this test, 10 g powder sample passed through a 2mm sieve after grinding was placed in a jar, and 50 mL distilled water was added. An Orion DUAL STAR pH meter was used to measure the pH value of the clear liquid [31].

For XRD, SEM, and MIP analyses, the broken samples after the measurement of 28-day compressive strength were collected. The samples were immersed in isopropyl alcohol for 7 days to terminate the hydration process [32]. Then, they were dried in a vacuum desiccator. XRD analysis was carried out on a diffractometer (Germany Bruker D8 Advance) with Cu-Kα radiation (k = 0.154 nm) at 40 kV and 40 mA over the 2θ range of 5°–75° with a step size of 0.01°. Before SEM observation, the samples were gold coated. The microstructures of the specimens were revealed by high resolution scanning electron microscope (HRSEM, Thermo APREO S A5-112). MIP was performed to test the porosity and pore structure distribution of samples (particle size of 2~3 mm), using an Auto Pore IV9500 mercury injection machine.

3. Experimental results

3.1. Properties of the fresh grouting material. Figure 3 presents the results of consistency and fluidity of the waste sediment-based grouting material with different mass concentrations of solid components. A decreased mass concentration led to continuously increased consistency and fluidity. In S1 (mass concentration of 69%), the consistency and fluidity were 91 mm and 145 mm, respectively, which significantly increased to 140 mm and 199 mm after decreasing the mass concentration to 61% (S5). When the mass concentration decreased, the water film thickness on the surface of the raw material particles increased, resulting in improved consistency and fluidity of the freshly mixed grouting material [9, 33]. In the construction field, the fluidity needs to be higher than 160 mm, and the consistency is suggested to be in the range of 100-130 mm [34]. Based on the results, the working performance of the fresh grouting material can meet the requirements when the mass concentration is within 63% to 67%.

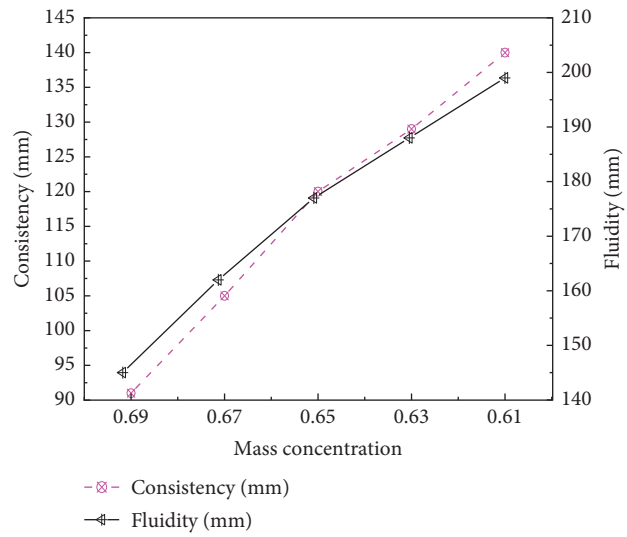

Figure 3: The consistency and fluidity of the waste sediment-based grouting material with different mass concentrations of solid components.

Based on sample S3 (mass concentration of 65%), the influence of binder to WS ratio on the consistency and fluidity of the waste sediment-based grouting material was analyzed, and the results are displayed in Figure 4. When the binder to WS ratio decreased, the consistency and fluidity of the grouting material also decreased. For sample S6 (binder to WS ratio of 2/1), the consistency and fluidity were 126 mm and 185 mm, respectively, which significantly changed to 97 mm and 159 mm at a binder to WS ratio of 1/6 (S11). Compared with cement particles, waste sediment particles are finer and have a high water absorption rate, increasing the water demand of the fresh slurry. An increased waste sediment amount causes the water film thickness on the surface of the raw material particles to decrease, leading to decreased consistency and fluidity [35, 36]. Considering both working property and price, the suitable binder to WS ratio is suggested to be in the range of 1/3-1/5.

Among the differentsamples, S9 (mass concentration of 65% and binder to WS ratio of 1/4) had a consistency of 106 mm and a fluidity of 165 mm, which was suitable for

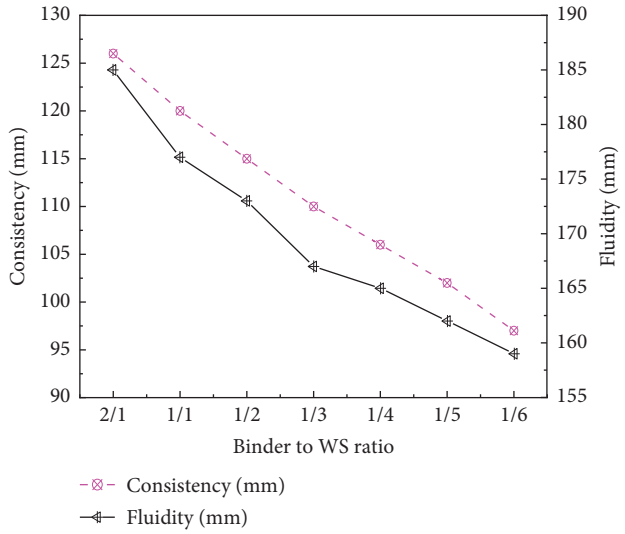

Figure 4: The consistency and fluidity of the waste sediment-based grouting material with different binders to WS ratios.

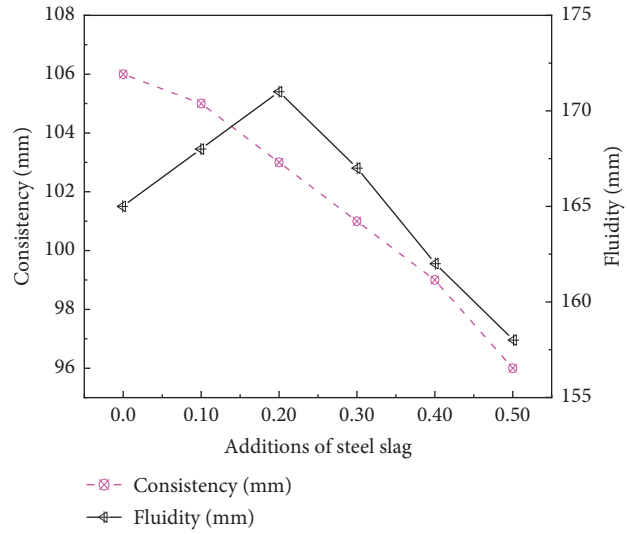

Figure 5: The consistency and fluidity of the waste sediment-based grouting material with different addition amounts of steel slag.

grouting engineering. Based on S9, the industrial waste-steel slag was utilized in the waste sediment-based grouting material. Figure 5 presents the consistency and fluidity of the waste sediment-based grouting material with different addition amounts of steel slag. The consistency of the fresh slurry continuously decreased with increase in the dosage of steel slag from 0% to 50%. The fluidity increased first from 165 mm (S9- 0% SL) to 171 mm (S13- 20% SL), and further additions of steel slag resulted in a slightly decreased fluidity. In fresh cement-based material, the fluidity is related to the particle shape and particle surface, while the consistency is related to the force between the particles [33]. Hence, steel slag has a different effect on the fluidity and consistency. The particle size distribution of steel slag is different from that of OPC. Adding an appropriate amount of steel slag can improve the particle gradation of raw materials and increase the fluidity [37, 38]. When the addition amount of steel slag was excessive, the fluidity was further reduced. The viscosity between the steel slag particles is larger than that of the OPC particles. The partial replacement of OPC by steel slag thickens the slurry and decreases the consistency value [39, 40].

Table 5 lists the setting time of the waste sediment-based grouting material. For the fresh slurry, decrease in mass concentration led to continuous increase in setting time. The setting time changed from 780 min (S1- mass concentration of 69%) to 870 min (S5- mass concentration of 61%). Decreased mass concentration results in a cumulatively reduced cementitious component and a prolonged hardening period[17]. When the binder to WS ratio changed from 2/1 to 1/6, the setting time significantly increased from 750 min (S6- binder to WS ratio of 2/1) to 1020 min (S11- binder to WS ratio of 1/6). In cement-based material, an increased sand-to-binder ratio is related to a decreased proportion of cementitious component, which leads to an increased setting time [10]. As shown in Table 5, successive additions of steel slag led to a slightly prolonged setting time. For S9 (0% SL),

Table 5: The setting time of the waste sediment-based grouting material.

Group	S1	S2	S3	S4	S5	S6	S7	S8
Setting time (min)	780	810	840	860	870	750	900	940
	S9	S10	S11	S12	S13	S14	S15	S16
Setting time (min)	970	1000	1020	980	1000	1020	1050	1080

the setting time was 970 min, which increased to 1080 min after adding 50% SL (S16). Since the reactivity of steel slag is lower than that of OPC in cement-based material, the incorporation of steel slag decreased the hydration rate in the waste sediment-based grouting material, resulting in a prolonged setting time [41].

Figure 6 presents the bleeding ratio and stone ratio of the waste sediment-based grouting material with different mass concentrations of solid components. A decrease in mass concentration led to a continuous increase in bleeding ratio and decrease in stone ratio. For S1 (mass concentration of 69%), the bleeding and stone ratios were 0.4% and 99.2%, respectively, which significantly changed to 1.9% and 95.4% at 61% mass concentration (S5). When the mass concentration decreased, the amount of cementitious components was reduced, and the setting time was prolonged [42, 43]. For the hardening slurry, the bleeding ratio was increased, and the stone ratio was decreased. The stone ratio needs to be higher than 95.0% for the construction field, and these five sample groups from S1 to S5 all meet this engineering requirement.

Based on S3, the influence of binder to WS ratio on the bleeding ratio and stone ratio of the waste sediment-based grouting material was analyzed, and the results are displayed in Figure 7. A decrease in binder to WS ratio led to a continuous increase in bleeding ratio and decrease in stone ratio. For S6 (binder to WS ratio of 2/1), the bleeding and

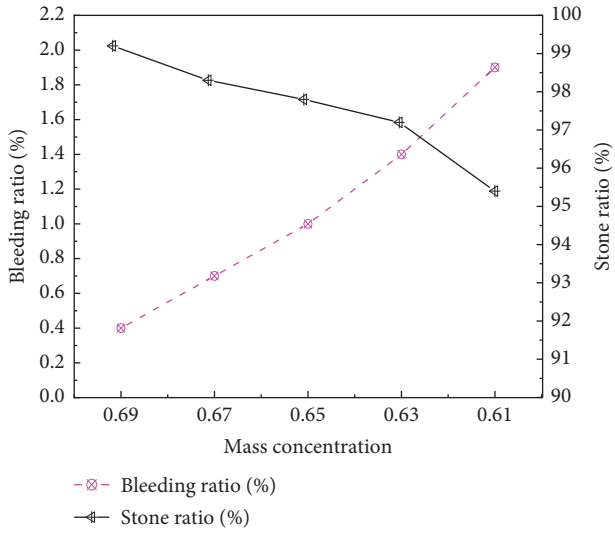

Figure 6: The bleeding ratio and stone ratio of the waste sediment-based grouting material with different mass concentrations of solid components.

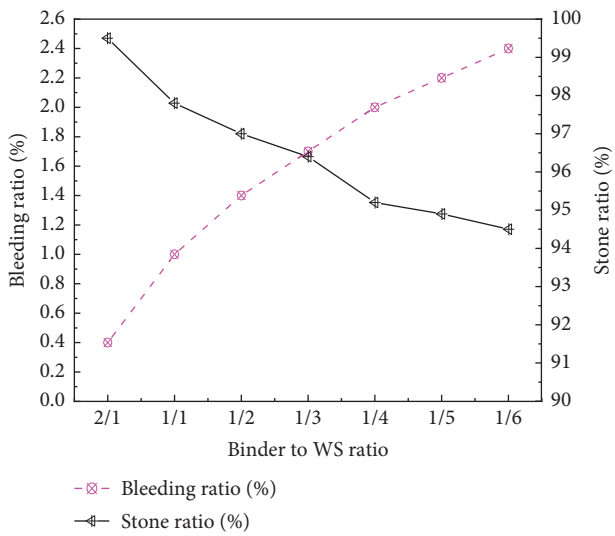

Figure 7: The bleeding ratio and stone ratio of the waste sediment-based grouting material with different binders to WS ratios.

stone ratios were 0.4% and 99.5%, respectively, which significantly changed to 2.4% and 94.5% at a 1/6 binder to WS ratio (S11). For cement-based grouts, the increased sand to binder ratio is associated with reduced binding performance and prolonged setting time, resulting in an increased bleeding ratio and decreased stone ratio [12, 44].

Based on S9, the effect of steel slag addition on the bleeding ratio and stone ratio of the waste sediment-based grouting material was analyzed, and the results are displayed in Figure 8. The bleeding ratio of the fresh slurry decreased first from 2.0% (S9- 0% SL) to 1.6% (S13- 20% SL), and further addition of steel slag resulted in a slightly increased bleeding ratio. For the fresh slurry, a lower bleeding ratio during hardening was associated with a higher stone ratio

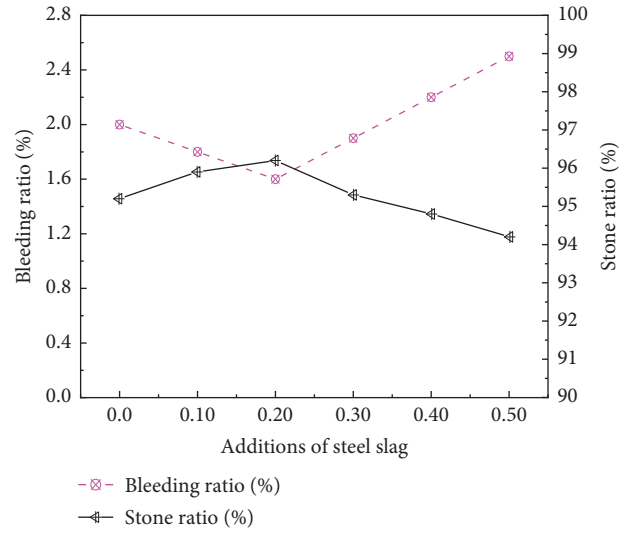

Figure 8: The bleeding ratio and stone ratio of the waste sediment-based grouting material with different addition amounts of steel slag.

after hardening. S13 (20% SL) had a stone ratio of 96.2%, which was the highest among the five groups. Although the alkalinity of steel slag is lower than that of OPC, adding an appropriate amount of steel slag can improve the cementitious property of the fresh slurry, resulting in decreased bleeding ratio and increased stone ratio [45, 46]. However, when the addition amount of steel slag is excessive, the binding property is further reduced.

Unlike the traditional cement and water glass-based grouting material, the waste sediment-based grouting material contains a high percentage of waste sediment and steel slag, which is eco-friendly. Besides, the waste sediment-based grouting material can achieve self-leveling and has a stone ratio over 95.0%, meeting the engineering requirement in subway construction.

3.2. Compressive strength of the waste sediment-based grouting material. Figure 9 presents the compressive strength of the waste sediment-based grouting material with different mass concentrations of solid components. At 3 days, the compressive strengths from S1 (mass concentration of 69%) to S5 (mass concentration of 61%) were 12.1 MPa, 10.5 MPa, 8.9 MPa, 7.5 MPa, and 6.6 MPa, respectively. At 28 days, the compressive strengths of these five sample groups were 21.5 MPa, 18.7 MPa, 16.5 MPa, 15.1 MPa, and 13.5 MPa, respectively. Decrease in mass concentration is associated with increased water content and decreased binder dosage, resulting in a continuousreduction in compressive strength [8, 47].

Figure 10 displays the effect of the binder to WS ratio on the compressive strength of the waste sediment-based grouting material. With the decrease in the binder to WS ratio, the utilization rate of the solid waste increases [48]. Besides, due to the decreased amount of OPC, the price and the performance of the synchronous grouting material reduces [29, 49]. As seen in Figure 10, for S6 (binder to WS

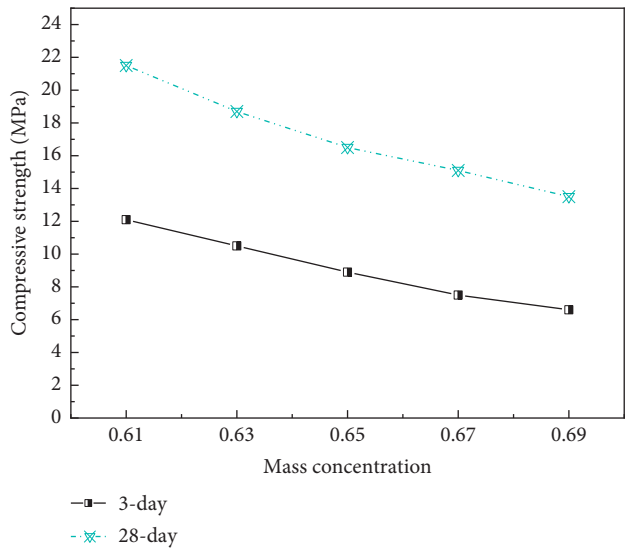

Figure 9: The compressive strength of the waste sediment-based grouting material with different mass concentrations of solid components.

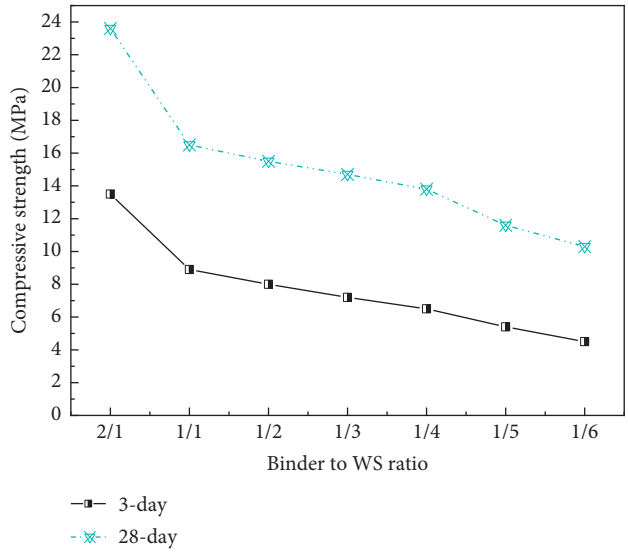

Figure 10: The compressive strength of the waste sediment-based grouting material with different binders to WS ratios.

ratio of 2/1), the 3-day and 28-day compressive strengths were 13.5 MPa and 23.6 MPa, respectively. When the binder to WS ratio decreased to 1/6 (S11), the 3-day and 28-day compressive strengths changed to 4.5 MPa and 10.3 MPa, respectively. At 28 days, the compressive strengths for samples S6 to S11 were 23.6 MPa, 15.5 MPa, 14.7 MPa, 13.8 MPa, 11.6 MPa, and 10.3 MPa, respectively. Considering both compressive strength and price, the optimal binder to WS ratio is in the range of 1/3-1/5.

Figure 11 presents the effects of SL content on the compressive strength of the waste sediment-based grouting material. Steel slag had a noticeable influence on compressive strength. With the increase in content of steel slag, the 3-day compressive strength decreased slightly. The 3-day

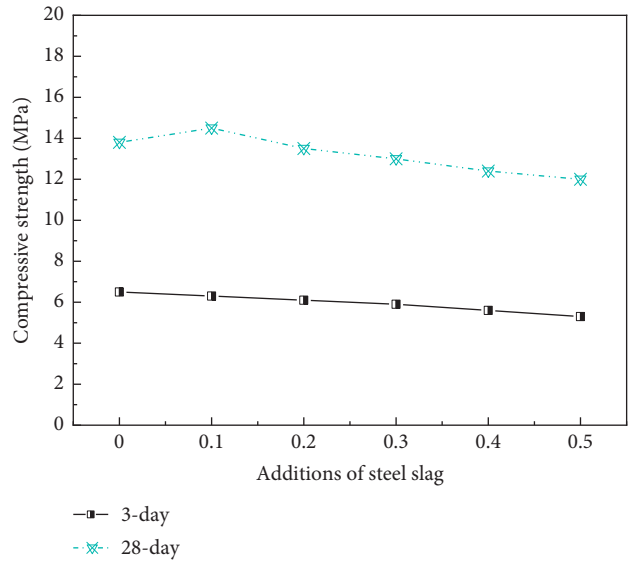

Figure 11: The compressive strength of the waste sediment-based grouting material with different addition amounts of steel slag.

strength values for the samples from S9 (0% SL) to S16 (50% SL) were 6.5 MPa, 6.3 MPa, 6.1 MPa, 5.9 MPa, 5.6 MPa, and 5.3 MPa, respectively. After curing for 28 days, the strength values from S9 (0% SL) to S16 (50% SL) were 13.8 MPa, 14.5 MPa, 13.5 MPa, 13.0 MPa, 12.4 MPa, and 12.0 MPa, respectively. S12 (10% SL) had the highest compressive strength among these groups at 28 days. This result showed that incorporating steel slag decreased the 3-day compressive strength, while a small amount of steel slag (around 10%) improved the 28-day compressive strength. In the current research, steel slag has a lower reactivity than OPC. Thus, the early strength (3-day) was reduced after incorporating steel slag. The active phases in steel slag can gradually hydrate and improve the cementitious property of the hardened matrix, leading to a slightly increased 28-day compressive strength [46, 50]. Besides, steel slag has a smaller particle size than OPC and achieves a pore-filling effect in the hardened grouting material [49]. Thus, the sample containing 10% steel slag possessed higher strength than other samples. However, the excessive addition of steel slag reduced the formation of main hydration phases and weakened the overall gelling properties. Thus, the compressive strength decreased again.

3.3. The pH value of the waste sediment-based grouting material. Table 6 lists the pH values of the waste sediment-based grouting material. The pH value of the hardened grouting material reduced slightly with the decrease in mass concentration of solid components, from 11.0 (S1- mass concentration of 69%) to 10.7 (S5- mass concentration of 61%). An alkaline environment is vital for the strength development of cement-based grouting material. Commonly, a higher pH value corresponds to a higher compressive strength [31]. In this research, the pH value development of the waste sediment-based grouting material with different mass concentrations was correlated with the

Table 6: The pH value of the waste sediment-based grouting material.

Group	S1	S2	S3	S4	S5	S6	S7	S8
pH value	11.0	10.9	10.8	10.8	10.7	11.4	10.5	10.3
	S9	S10	S11	S12	S13	S14	S15	S16
pH value	10.2	10.1	10.1	10.0	9.9	9.7	9.6	9.5

strength value. Based on S3, when the binder to WS ratio was varied from 2/1 to1/6, the pH value of the fresh slurry significantly decreased from 11.4 (S6- binder to WS ratio of 2/1) to 10.1 (S11- binder to WS ratio of 1/6). As shown in Table 2, the waste sediment had a near-neutral pH value (6.91). Thus, the partial replacement of OPC by waste sediment decreased the pH value of the hardened grouting material [51, 52]. As shown inTable 1, steel slag contains 46.11% CaO, 15.36% SiO_2, 18.02% Fe_2O_3, and 9.91% MgO. It is less alkaline than OPC [53]. Hence, adding steel slag resulted in a decreased pH value. When the dosage of steel slag was increased from 0% to 50%, the pH value of the hardened grouting material slightly changed from 10.2 (S9- 0% SL) to 9.5 (S16- 50% SL).

4. Mechanism discussion

4.1. XRD analysis. Figure 12 presents the XRD patterns of waste sediment and hardened waste sediment-based grouting material after curing for 28 days. In the untreated waste sediment, the diffraction peaks of crystal minerals such as quartz, kaolinite, and illite were clearly observed in the range of 19-35°. For the hardened waste sediment-based grouting material shown in Figure 12(b)–12(d), a relatively broad diffraction peak of amorphous minerals was observed in the range of 22~32°, indicating the formation of amorphous gel phases in the grouting material [54].

Comparedwith the XRD pattern of waste sediment, the diffraction peak intensity of kaolinite, illite, and quartz decreased significantly, while the peak intensity of zeolite and ettringite increased correspondingly in the XRD pattern of waste sediment-based grouting material. Moreover, the diffraction peak of quartz crystal in hardened sample also decreased slightly in intensity. These resultsindicated that some active minerals in waste sediment were consumed by chemical reaction (pozzolanic reaction), which generated a small amount of cementitious hydrates together with the reaction of cement and steel slag, thus enhancing the compressive strength of the grouting material. However, no diffraction peaks of calcium hydroxide crystal were detected for the hardened sample.

The reaction between OPC and steel slag is based on breaking Si-O, Al-O, and Ca-O bonds inside vitreous steel slag by OH– ions, which leads to the formation of CSH-like products [25]. When calcium hydroxide is consumed in this reaction, the durability and compressive strength of hardened sample are enhanced [28, 55]. This is the mechanism by which steel slag improves the mechanical properties in the OPC-steel slag-waste sediment system. Herein, the strength development of hardened waste sediment-based grouting material can be attributed to the formation of hydration products and the cementation between hydrates and sediment particles.

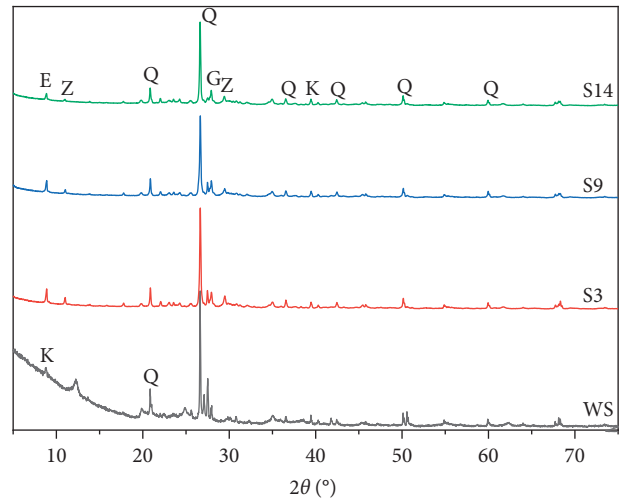

Figure 12: XRD patterns of hardened waste sediment-based grouting material after curing for 28 days: (a) S1; (b) S3; (c) S9; and (d) S14. (q) quartz, (e) ettringite, (z) zeolite, (g) gismondine, (k) kaolinite)

4.2. SEM analysis. Figure 13 displays the SEM images of hardened waste sediment-based grouting material after curing for 28 days. As shown in Figure 1(c), the waste sediment presented a wide particle size distribution. There were many irregular particles of different sizes, with a diverse particle morphology and rough surface. Thus, the waste sediment exhibited a high-water absorption ratio when preparing the grouting material [19, 29]. This can explain the results of decreased consistency and fluidity with decrease in the binder to WS ratio. Compared with Figure 13(b), there were more needle-like and flocculated C-S-H gels in the hardened sample prepared by a 1/1 binder to WS ratio (S3), as shown in Figure 13(a). The needle-shaped gels were also observed among the waste sediment particles, leading to a denser interlocked structure. As the binder to WS ratio decreased, the gelatinous phases and flocculent products reduced, and the amount of unreacted waste sediment particles increased. Due to the decrease in OPC content, the amount of cementitious products was reduced. This led to weaker adhesion between the particles in the microstructure, resulting in decreased compressive strength [40].

Figure 13(c) shows that adding 10% steel slag can improve the cementitious property in the waste sediment-based grouting material. Compared with S9, the particles were bonded more tightly in S12. Yang et al. [37] found that adding a suitable amount of steel slag can improve the compressive strength by promoting the hydration rate in cement-based material. Adding 10% steel slag improved the particle size distribution of the grains. Besides, steel slag reacted with the calcium hydroxide produced by OPC, which promoted the hydration degree and increased the property of cement matrix. This created a synergistic

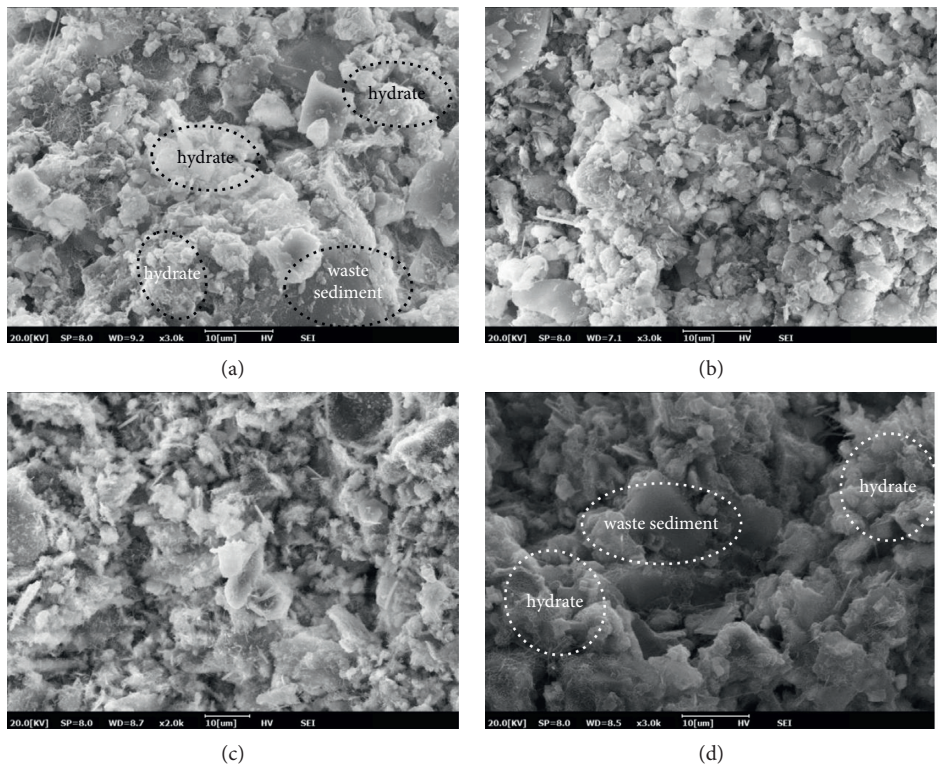

Figure 13: SEM images of hardened waste sediment-based grouting material after curing for 28 days: (a) S3; (b) S9; (c) S12; and (d) S14.

promotion effect between steel slag and cement, resulting in better mechanical properties. As shown in Figure 13(d), more honeycomb gel phases were formed in the sample containing 30% steel slag (S14). Steel slag has a lower reactivity than OPC. At 3 days, the compressive strength of the hardened sample containing steel slag decreased. However, steel slag can react slowly. At 28 days, many hydrates can be formed by steel slag [40, 54]. The hydration product of OPC and steel slag tightly connected the inert waste sediment particles, leading to a 28-day compressive strength of 13.0 MPa. This strength canmeet the performance requirements of synchronous grouting materials in shield tunnel construction [56]. These results indicate that the steel slag incorporated with OPC binder was superior to OPC in stabilizing high-water content waste sediment, especially in the long-term property development.

4.3. MIP analysis. Figure 14 displays the MIP results of hardened waste sediment-based grouting material after curing for 28 days. It can be seen that the total porosity values of S1, S3, S9, S12, and S14 were 16.30%, 17.12%, 18.21%, 17.49%, and 17.79%, respectively. The decreased mass concentration was related to increased water addition. Hence, the porosity increased from 16.30% (S1-69% mass concentration) to 18.21% (S3-65% mass concentration). Ma et al. [32] pointed out that the compressive strength of OPC-based materials is inversely proportional to the total porosity. Changing the binder to WS ratio from 1:1 to 1:4

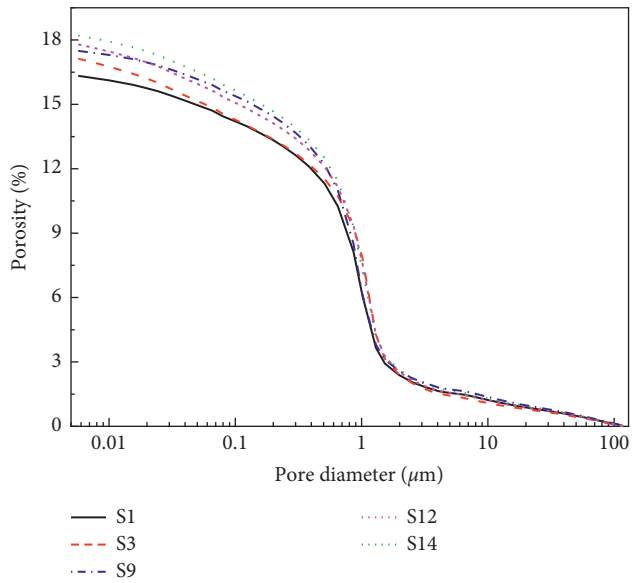

Figure 14: MIP results of hardened waste sediment-based grouting material after curing for 28 days.

caused a looser microstructure and lower compressive strength. Moreover, the porosity slightly increased from 17.12% to 18.21%.

The porosity values of the sample after adding 0%, 10%, and 30% steel slag were 18.21%, 17.49%, and 17.79%, respectively. As shown in Figure 1, steel slag has a smaller particle size than OPC. Adding a suitable amount of fine

steel slag particles modified the microstructure of waste sediment-based grouting material by the pore-filling effect, leading to increased strength [43]. However, steel slag has a lower reactivity than OPC. Excessive addition of steel slag could reduce the amount of cementitious hydration products formed in the matrix, causing a decrease in the bonding force [57]. Compared with S12 (10% steel slag), the strength of S14 (30% steel slag) was reduced. Thus, the MIP results were consistent with the above analysis.

5. Conclusion

In this work, waste sediment was upcycled to prepared grouting material. The main properties of the waste sediment-based grouting material were studied by varying the mass concentration of solid components, binder to WS ratio, and steel slag addition. The main conclusions of this work are as follows:

(1) The decrease in mass concentration of solid components from 69% (S1) to 61% (S5) led to improved working performances (consistency, fluidity, setting time, bleeding ratio), while decrease in binder to WS ratio from 2/1 (S6) to 1/6 (S11) caused poorer working performances. Both decreased mass concentration and binder to WS ratio led to reduced compressive strength and lower pH value of the hardened sample.

(2) Steel slag has a smaller particle size and lower reactivity than OPC. Successive additions of steel slag from 0% (S9) to 50% (S16) resulted in decreased consistency and increased setting time. The fluidity and stone ratio increased first and then decreased, reaching the maximum when the dosage was 20% (S13). The 28-day compressive strength of the hardened sample also increased first and then decreased, reaching the maximum at 10% addition amount of steel slag (S12).

(3) The waste sediment-based grouting material exhibited superior performance to traditional grouting materials. It achieved self-leveling (160 mm fluidity), and was suitable for grouting (consistency within 100-130 mm, 95.0% stone ratio). The 1-day and 28-day compressive strength reached 6.5 MPa and 13.5 MPa, respectively. High-volume waste sediment was upcycled to prepare the grouting material, which is beneficial to the environment.

(4) Some amorphous phases were formed in the waste sediment-based grouting material. The strength development of the grouting material can be attributed to the formation of hydration products and the cementation between hydrates and sediment particles. The addition of a suitable amount of steel slag (10%) can reduce the total porosity of the hardened sample. Steel slag reacted with the calcium hydroxide produced by OPC, which promoted the hydration degree and increased the mechanical properties of cement matrix.

Data Availability

The data used to support the findings of this study are plotted within the article, and the raw data files are available by contacting the corresponding author.

Conflicts of Interest

The authors declare that there are no conflicts of interest.

Acknowledgments

This research was supported by the Doctoral Research Start-up Fund of Shandong Jiaotong University (Grant No. 50004930).

References

[1] C. Zhang, J. Yang, J. Fu, S. Wang, J. Yin, and Y. Xie, "Recycling of discharged soil from EPB shield tunnels as a sustainable raw material for synchronous grouting," *Journal of Cleaner Production*, vol. 268, Article ID 121947, 2020.

[2] M. Gao, J. Xie, Y. Gao et al., "Mechanical behavior of coal under different mining rates: a case study from laboratory experiments to field testing," *International Journal of Mining Science and Technology*, vol. 31, no. 5, pp. 825–841, 2021.

[3] Y. Zhanhu, Z. Boyang, C. Yu, S. Hailong, and T. Yi, "Study and application of synchronous grouting techniques in the launching section of an extra-large diameter shield tunnel," *Modern Tunnelling Technology*, vol. 52, no. 4, pp. 101–104, 2015.

[4] S. Li, X. Wang, Z. Xu, D. Mao, and D. Pan, "Numerical investigation of hydraulic tomography for mapping karst conduits and its connectivity," *Engineering Geology*, vol. 281, p. 105967, 2021.

[5] D. Chen, H. Chen, W. Zhang, J. Lou, and B. Shan, "An analytical solution of equivalent elastic modulus considering confining stress and its variables sensitivity analysis for fractured rock masses," *Journal of Rock Mechanics and Geotechnical Engineering*, 2021.

[6] C. Ma, Y. Liu, H. Zhou et al., "Influencing mechanism of sodium tripolyphosphate on the rheological properties of magnesium phosphate cement," *Powder Technology*, vol. 387, pp. 406–414, 2021.

[7] C. Ma, Y. Liu, H. Zhou, Z. Jiang, W. Ren, and F. He, "Influencing mechanism of mineral admixtures on rheological properties of fresh magnesium phosphate cement," *Construction and Building Materials*, vol. 288, Article ID 123130, 2021.

[8] J. Zhang, S. Li, Z. Li, C. Liu, Y. Gao, and Y. Qi, "Properties of red mud blended with magnesium phosphate cement paste: feasibility of grouting material preparation," *Construction and Building Materials*, vol. 260, Article ID 119704, 2020.

[9] L. Han, L. Wang, X. Ding, H. Wen, X. Yuan, and W. Zhang, "Similarity quantification of soil parametric data and sites using confidence ellipses," *Geoscience Frontiers*, vol. 13, Article ID 101280, 2021.

[10] M. R. Azadi, A. Taghichian, and A. Taheri, "Optimization of cement-based grouts using chemical additives," *Journal of Rock Mechanics and Geotechnical Engineering*, vol. 9, no. 4, pp. 623–637, 2017.

[11] C. Cao, W. Zhang, J. Chen, B. Shan, S. Song, and J. Zhan, "Quantitative estimation of debris flow source materials by integrating multi-source data: a case study," *Engineering Geology*, vol. 291, Article ID 106222, 2021.

[12] Y. Liu and B. Chen, "Research on the preparation and properties of a novel grouting material based on magnesium phosphate cemen," *Construction and Building Materials*, vol. 214, pp. 516–526, 2019.

[13] C. Zhu, Z. Yan, Y. Lin, F. Xiong, and Z. Tao, "Design and application of a monitoring system for a deep railway foundation pit project," *Ieee Access*, vol. 7, pp. 107591–107601, 2019.

[14] M. Amar, M. Benzerzour, and N.-E. Abriak, "Towards the establishment of formulation laws for sediment-based mortars," *Journal of Building Engineering*, vol. 16, pp. 106–117, 2018.

[15] M. Gao, H. Hao, S. Xue et al., "Discing behavior and mechanism of cores extracted from Songke-2 well at depths below 4,500 m," *International Journal of Rock Mechanics and Mining Sciences*, vol. 149, p. 104976, 2022.

[16] M. Amar, M. Benzerzour, N.-E. Abriak, and Y. Mamindy-Pajany, "Study of the pozzolanic activity of a dredged sediment from Dunkirk harbour," *Powder Technology*, vol. 320, pp. 748–764, 2017.

[17] R. Liu, Z. Zheng, L. Shucai, and Q. Zhang, "Study on grouting penetration in soil rock mixture and the mechanical behavior after grouting reinforcement," *Journal of Testing and Evaluation*, vol. 47, no. 3, pp. 2240–2254, 2019.

[18] K. Gu and B. Chen, "Loess stabilization using cement, waste phosphogypsum, fly ash and quicklime for self-compacting rammed earth construction," *Construction and Building Materials*, vol. 231, Article ID 117195, 2020.

[19] M. Amar, M. Benzerzour, J. Kleib, and N.-E. Abriak, "From dredged sediment to supplementary cementitious material: characterization, treatment, and reuse," *International Journal of Sediment Research*, vol. 36, no. 1, pp. 92–109, 2021.

[20] C. Zhu, K. Zhang, H. Cai et al., "Combined application of optical fibers and CRLD bolts to monitor deformation of a pit-in-pit foundation," *Advances in Civil Engineering*, vol. 2019, pp. 1–16, Article ID 2572034, 2019.

[21] S. Celik, "An experimental investigation of utilizing waste red mud in soil grouting," *Ksce Journal of Civil Engineering*, vol. 21, no. 4, pp. 1191–1200, 2017.

[22] A. Bayat, A. Hassani, and A. A. Yousefi, "Effects of red mud on the properties of fresh and hardened alkali-activated slag paste and mortar," *Construction and Building Materials*, vol. 167, pp. 775–790, 2018.

[23] L. Wang, I. K. M. Yu, D. C. W. Tsang et al., "Transforming wood waste into water-resistant magnesia-phosphate cement particleboard modified by alumina and red mud," *Journal of Cleaner Production*, vol. 168, pp. 452–462, 2017.

[24] L. Han, L. Wang, W. Zhang, B. Geng, and S. Li, "Rockhead profile simulation using a simplified generation method of conditional random field," *Journal of Rock Mechanics and Geotechnical Engineering*, vol. 2021, 2021.

[25] R. Achour, R. Zentar, N.-E. Abriak, P. Rivard, and P. Gregoire, "Durability study of concrete incorporating dredged sediments," *Case Studies in Construction Materials*, vol. 11, p. e00244, 2019.

[26] C. Zhang, J. Fu, J. Yang, X. Ou, X. Ye, and Y. Zhang, "Formulation and performance of grouting materials for underwater shield tunnel construction in karst ground," *Construction and Building Materials*, vol. 187, pp. 327–338, 2018.

[27] X. Man, M. A. Haque, and B. Chen, "Engineering properties and microstructure analysis of magnesium phosphate cement mortar containing bentonite clay," *Construction and Building Materials*, vol. 227, Article ID 116656, 2019.

[28] Y. Cui and Z. Tan, "Experimental study of high performance synchronous grouting materials prepared with clay," *Materials*, vol. 14, no. 6, p. 1362, 2021.

[29] Y. Maierdan, M. A. Haque, B. Chen, M. Maimaitiyiming, and M. R. Ahmad, "Recycling of waste river sludge into unfired green bricks stabilized by a combination of phosphogypsum, slag, and cement," *Construction and Building Materials*, vol. 260, p. 120666, 2020.

[30] Z. Guijin, Y. Dongsheng, L. Jingwei, Z. Cong, and P. Ye, "Study on strength of clay-cement grouting material," *Water Resources and Hydropower Engineering*, vol. 46, no. 1, pp. 52–56, 2015.

[31] M. Cong, C. Longzhu, and C. Bing, "Analysis of strength development in soft clay stabilized with cement-based stabilizer," *Construction and Building Materials*, vol. 71, pp. 354–362, 2014.

[32] K. L. Scrivener, R. Snellings, and B. Lothenbach, *A Practical Guide to Microstructural Analysis of Cementitious Materials*, Taylor & Francis Group, LLC, Boca Raton, Florida, 2016.

[33] C. Ma, G. Chen, Z. Jiang et al., "Rheological properties of magnesium phosphate cement with different M/P ratios," *Construction and Building Materials*, vol. 282, p. 122657, 2021.

[34] Y. Zhang, S. Wang, B. Zhang et al., "A preliminary investigation of the properties of potassium magnesium phosphate cement-based grouts mixed with fly ash, water glass and bentonite," *Construction and Building Materials*, vol. 237, p. 117501, 2020.

[35] Y. Zhang, J. Wang, L. Li et al., "Basic properties and mechanism of high activity phosphate-based slurry for dynamic water blocking-A feasibility research," *Construction and Building Materials*, vol. 275, p. 122040, 2021.

[36] Z. Dou, S. Tang, X. Zhang et al., "Influence of shear displacement on fluid flow and solute transport in a 3D rough fracture," *Lithosphere*, vol. 2021, p. 1569736, 2021.

[37] Y. Jianming, L. Jingwen, W. Qisheng, X. M. Feng, and L. Xiaohua, "Influence of steel slag powders on the properties of MKPC paste," *Construction and Building Materials*, vol. 159, pp. 137–146, 2018.

[38] Y. Jiang, M. R. Ahmad, and B. Chen, "Properties of magnesium phosphate cement containing steel slag powder," *Construction and Building Materials*, vol. 195, pp. 140–147, 2019.

[39] S. Ali, S. Iqbal, S. Room, A. Ali, and Z. U. Rahman, "Value added usage of granular steel slag and milled glass in concrete production," *Journal of Engineering Research*, vol. 9, no. 1, pp. 73–85, 2021.

[40] B. Yuan, Z. Li, Z. Zhao, H. Ni, Z. Su, and Z. Li, "Experimental study of displacement field of layered soils surrounding laterally loaded pile based on transparent soil," *Journal of Soils and Sediments*, vol. 21, no. 9, pp. 3072–3083, 2021.

[41] L. Lang, C. Song, L. Xue, and B. Chen, "Effectiveness of waste steel slag powder on the strength development and associated micro-mechanisms of cement-stabilized dredged sludge," *Construction and Building Materials*, vol. 240, Article ID 117975, 2020.

[42] M. L. Gualtieri, M. Romagnoli, and A. F. Gualtieri, "Preparation of phosphoric acid-based geopolymer foams using limestone as pore forming agent - thermal properties by in situ XRPD and Rietveld refinements," *Journal of the European Ceramic Society*, vol. 35, no. 11, pp. 3167–3178, 2015.

[43] P. Labadie, A. B. Cundy, K. Stone, M. Andrews, S. Valbonesi, and E. M. Hill, "Evidence for the migration of steroidal estrogens through river bed sediments," *Environmental Science & Technology*, vol. 41, no. 12, pp. 4299–4304, 2007.

[44] Z. Mo, R. Wang, and X. Gao, "Hydration and mechanical properties of UHPC matrix containing limestone and different levels of metakaolin," *Construction and Building Materials*, vol. 256, p. 119454, 2020.

[45] J.-Q. Liu, K.-V. Yuen, W.-Z. Chen, X.-S. Zhou, and Wei-Wang, "Grouting for water and mud inrush control in weathered granite tunnel: a case study," *Engineering Geology*, vol. 279, Article ID 105896, 2020.

[46] Y. C. Lim, Y.-J. Shih, K.-C. Tsai, W.-D. Yang, C.-W. Chen, and C.-D. Dong, "Recycling dredged harbor sediment to construction materials by sintering with steel slag and waste glass: characteristics, alkali-silica reactivity and metals stability," *Journal of Environmental Management*, vol. 270, Article ID 110869, 2020.

[47] Y. Liu, Z. Qin, and B. Chen, "Experimental research on magnesium phosphate cements modified by red mud," *Construction and Building Materials*, vol. 231, Article ID 117131, 2020.

[48] B. Anger, I. Moulin, J.-P. Commene, F. Thery, and D. Levacher, "Fine-grained reservoir sediments: an interesting alternative raw material for Portland cement clinker production," *European Journal of Environmental and Civil Engineering*, vol. 23, no. 8, pp. 957–970, 2019.

[49] K. Gu, B. Chen, and Y. Pan, "Utilization of untreated-phosphogypsum as filling and binding material in preparing grouting materials," *Construction and Building Materials*, vol. 265, Article ID 120749, 2020.

[50] G. Hanqing, Y. Xiaoguang, Z. Chaoming, Y. Dadi, Z. Qi, and L. Zhongfei, "Application study of steel slag powder in cement based grouting material," *Concrete*, no. 2, pp. 85–87, 2014.

[51] H. Li, H. Zhang, L. Li et al., "Utilization of low-quality desulfurized ash from semi-dry flue gas desulfurization by mixing with hemihydrate gypsum," *Fuel*, vol. 255, Article ID 115783, 2019.

[52] Z. Dou, Y. Liu, X. Zhang et al., "Influence of layer transition zone on rainfall-induced instability of multilayered slope," *Lithosphere*, vol. 2021, Article ID 2277284, 4 pages, 2021.

[53] E. Adesanya, K. Ohenoja, A. Di Maria, P. Kinnunen, and M. Illikainen, "Alternative alkali-activator from steel-making waste for one-part alkali-activated slag," *Journal of Cleaner Production*, vol. 274, Article ID 123020, 2020.

[54] J. Wang, J. Xie, Y. Wang, Y. Liu, and Y. Ding, "Rheological properties, compressive strength, hydration products and microstructure of seawater-mixed cement pastes," *Cement and Concrete Composites*, vol. 114, Article ID 103770, 2020.

[55] S. Rehman, S. Iqbal, and A. Ali, "Combined influence of glass powder and granular steel slag on fresh and mechanical properties of self-compacting concrete," *Construction and Building Materials*, vol. 178, pp. 153–160, 2018.

[56] J. Wang and E. Liu, "Upcycling waste seashells with cement: rheology and early-age properties of Portland cement paste," *Resources, Conservation and Recycling*, vol. 155, Article ID 104680, 2020.

[57] K. K. Aligizaki, *Pore Structure of Cement-Based Materials: Testing, Interpretation and Requirements*, Taylor & Francis, London and New York, 2006.